PHYSICAL REVIEW D **92,** 074008 (2015)

Insights into $Q^2\bar{Q}^2$ states from an effective perspective

Ll. Ametller[1] and P. Talavera[2]

[1]*Departament de Física i Enginyeria Nuclear, Universitat Politècnica de Catalunya, Jordi Girona 5, E-08034 Barcelona, Spain*

[2]*Universitat Internacional de Catalunya, Immaculada 22, E-08017 Barcelona, Spain*

(Received 24 April 2015; revised manuscript received 3 August 2015; published 7 October 2015)

We discuss the two-photon coupling of the lightest scalar meson on the basis of an extension of χPT. Using low-energy data on the pion form factor and the $\gamma\gamma \to \pi^+\pi^-(\pi^0\pi^0)$ cross sections as inputs, we find $\Gamma(\sigma \to \gamma\gamma) \cong 0.126$ keV. The smallness of the result and the relative weight between its components, $\frac{\Gamma_{\gamma\gamma\to S_1}}{\Gamma_{\gamma\gamma\to\pi\pi\to S_1}} \leq 1$, suggests that the scalar 0^{++} meson is mainly a $Q^2\bar{Q}^2$ state.

DOI: 10.1103/PhysRevD.92.074008 PACS numbers: 13.20.Jf, 11.30.Rd, 12.39.Fe, 12.38.Aw

I. INTRODUCTION

The plethora of scalar mesons in QCD has a long and puzzling history. Probably, due to its elusiveness, the most interesting state is the isoscalar $I = 0$, $\sigma(600)$ [1]. It is well known as a broad enhancement in very low-energy s-wave meson-meson scattering. The quark or gluon content of the $\sigma(600)$ is not fully understood, and the proliferation of models with seemingly different conclusions is disturbing [2,3]. At the same time, its underlying structure is a cornerstone in understanding the realization of the mechanism for chiral symmetry breaking.

In this paper, we find indications of the $Q^2\bar{Q}^2$ content for the σ state and estimate it by studying the processes $\gamma\gamma \to \pi\pi$ and the pion vector form factor. The tetraquark structure of the lightest scalar was proposed a long time ago, owing to a possible strong diquark correlation [4]. Our working framework runs in parallel to that in Ref. [5] with the only difference being that we interpret their Lagrangian in an effective perspective by providing a counting power to the singlet field [6]. Our main result is based on the comparison of two terms: the first one, already studied in Ref. [7], is given by the rescattering effects contribution to the $\gamma\gamma \to \pi\pi \to S_1$ decay, and the second is given by the direct $\gamma\gamma \to S_1$ coupling. At the fundamental level, the two-photon coupling for a generic S_1 scalar meson is given by

$$\mathcal{L} = -\frac{e^2}{4F} c_{1\gamma} S_1 F_{\mu\nu} F^{\mu\nu}. \tag{1}$$

There are many ways to couple the scalar singlet to the vacuum. If one considers that the spontaneous breaking of scale invariance is mediated via the trace of the energy-momentum tensor, the coupling $c_{1\gamma}$ is related to the scalar decay constant via the relation [8]

$$-\frac{e^2}{4F} c_{1\gamma} F_{S_1} = \frac{\alpha}{6\pi} \frac{\sigma(e^+e^- \to \text{hadrons})}{\sigma(e^+e^- \to \mu^+\mu^-)}$$
$$\text{and} \quad \langle 0|\theta^\mu_\mu|S_1\rangle = -M^2_{S_1} F_{S_1}, \tag{2}$$

with θ^μ_μ the trace of the energy momentum tensor

$$\theta^\mu_\mu := \theta_g + \theta_q = \frac{1}{4}\beta(\alpha_s) G^a_{\mu\nu} G^{\mu\nu a} + \sum_i m_i \bar{\psi}_i (1 + \gamma_m(\alpha_s))\psi_i. \tag{3}$$

Instead, if we consider that the scalar meson is an S-wave bound state of the diquark-antidiquark pair, the corresponding interpolating field can be constructed as

$$j_\sigma = \epsilon_{abc}\epsilon_{dec}(u^T_a C\gamma_5 d_b)(\bar{u}_d \gamma_5 C \bar{d}^T_e), \tag{4}$$

where Latin indices denote color and C stands for the charge conjugation matrix. In the above expression, the diquark is taken to be a spin-zero color antitriplet and flavor antitriplet [9]. Then, the coupling to the vacuum is given by [10]

$$\langle 0|j_\sigma|S_1\rangle = -\sqrt{2} M^4_{S_1} F_{S_1}. \tag{5}$$

II. SETTING THE SCHEME

Let us first recall the main ingredients of the theoretical setup. We shall consider an effective approach to QCD with two flavors in the isospin limit. The smallness of the values of the light-quark masses and the external momenta set a perturbative scheme out of the chiral symmetry limit. We count the pion and scalar field as $\mathcal{O}(p^0)$; derivatives, vector, and axial-vector external currents as $\mathcal{O}(p)$; and the scalar, pseudoscalar external currents, and scalar mass as $\mathcal{O}(p^2)$. With this counting, the leading-order Lagrangian reduces to that presented in Ref. [11]:

$$\mathcal{L}_2[0^{++}] = \left(\frac{F^2}{4} + F c_{1d} S_1 + c_{2d} S_1^2 + \cdots\right)\langle u^\dagger_\mu u^\mu\rangle + \left(\frac{F^2}{4} + F c_{1m} S_1 + c_{2m} S_1^2 + \cdots\right) \times (\langle\chi_+\rangle - \langle\chi^\dagger + \chi\rangle). \tag{6}$$

The pseudoscalar field is parametrized by the unitary matrix $u(x)^2 = U(x) = e^{i\sqrt{2}\sum_j \sigma_j \phi_j(x)/F}$. Here, F is the pion decay constant ($F \simeq 93$ MeV), the ϕ_i's are fields for the pseudoscalar Goldstone mesons, and σ_i are the Pauli matrices. The basic building blocks are defined as

$$\begin{aligned}\chi &= 2B_0(s+ip),\\ u_\mu &= iu^\dagger D_\mu U u^\dagger = -iuD_\mu U^\dagger u = u_\mu^\dagger,\\ \chi_+ &= u^\dagger \chi u^\dagger + u\chi^\dagger u. \end{aligned} \tag{7}$$

Next-to-leading-order corrections, $\mathcal{O}(p^4)$, come either through one-loop graphs or by higher-order operators. In particular, the terms relevant to our study are explicitly[1]

$$\begin{aligned}\mathcal{L}_4[0^{++}] = &\sum_{i=5}^{6} \ell_i P_i + Z_1 \mathring{M}_\sigma^2 \langle \chi^\dagger U + \chi U^\dagger\rangle \\ &+ Z_2 \mathring{M}_\sigma^2 \langle D_\mu U D^\mu U^\dagger\rangle - \frac{e^2}{4F} c_{1\gamma} S_1 F_{\mu\nu} F^{\mu\nu}, \end{aligned} \tag{8}$$

where $\mathring{M}_\sigma$ stands for the singlet mass in the chiral limit and

$$P_5 = -\frac{1}{2}\langle f_-^{\mu\nu} f_{-\mu\nu}\rangle, \qquad P_6 = \frac{i}{4}\langle f_+^{\mu\nu}[u_\mu, u_\nu]\rangle, \tag{9}$$

with $f_\pm^{\mu\nu} = uF_L^{\mu\nu}u^\dagger \pm u^\dagger F_R^{\mu\nu} u$. The field strength tensors $F_{L,R}^{\mu\nu}$ are related to the non-Abelian external fields [12]. One salient feature of the field theory approach presented above is that it allows us to separate between the direct and rescattering $\gamma\gamma$ couplings in a crystal clear fashion. The reason is that the direct process always involves the gauge-invariant operator in Eq. (8), $S_1 F_{\mu\nu}F^{\mu\nu}$. Such a separation is not always feasible using dispersion relations.

III. CHARGED PION-PAIR PRODUCTION

The amplitude for the process $\gamma(q,\lambda)\gamma(q',\lambda') \to \pi^+(p)\pi^-(p')$ is given by $\mathcal{A}(\lambda,\lambda') = e^2\epsilon^\mu(q,\lambda)\epsilon'^\nu(q',\lambda')V_{\mu\nu}^C$, where the $V_{\mu\nu}^C$ tensor can be decomposed into four Lorentz-invariant tensor structures, although by gauge invariance, only two of them have a nonvanishing contribution to the cross section

$$\begin{aligned} V_{\mu\nu}^C &= A^C(s,t,u)T_{1\mu\nu} + B^C(s,t,u)T_{2\mu\nu},\\ T_{1\mu\nu} &= \frac{s}{2}g_{\mu\nu} - q_\nu q'_\mu,\\ T_{2\mu\nu} &= 2s\Delta_\mu\Delta_\nu - \nu^2 g_{\mu\nu} - 2\nu(q_\nu\Delta_\mu - q'_\mu\Delta_\nu), \end{aligned} \tag{10}$$

with $s = (q+q')^2$, $t = (q-p)^2$, $u = (q-p')^2$, and $\Delta_\mu := (p-p')_\mu$. The amplitudes $A^C(s,t,u)$ and $B^C(s,t,u)$ are analytic functions of the Mandelstand variables and are symmetric under crossing $\{t,u\} \leftrightarrow \{u,t\}$. Comparison with the experimental data will be at the level of the cross section. The differential cross section for unpolarized photons can be casted in terms of the helicity amplitudes $H_{+\pm}^C$ corresponding to helicity changes $\lambda = 0, 2$, respectively,

$$\frac{d\sigma}{d\Omega} = \frac{\alpha^2 s}{32}\beta(s) H^C(s,t), \qquad H^C(s,t) = |H_{++}^C|^2 + |H_{+-}^C|^2. \tag{11}$$

In terms of the amplitudes A^C and B^C, they read

$$H_{++}^C = A^C + 2(4M_\pi^2 - s)B^C, \qquad H_{+-}^C = \frac{8(M_\pi^4 - tu)}{s}B^C. \tag{12}$$

At $\mathcal{O}(p^2)$, there is no scalar contribution, and the amplitude coincides with that of scalar electrodynamics. At $\mathcal{O}(p^4)$, we have found remarkably many more diagrams than in χPT. Their evaluation is rather straightforward, and the contributions can be conveniently cast in terms of two tensorial structures as

$$\begin{aligned}\mathcal{A}^{(4)} = &e^2 A(s,t,u)(s\epsilon\cdot\epsilon' - 2q\cdot\epsilon' q'\cdot\epsilon)\\ &+ e^2 B(s,t,u)\left(\epsilon\cdot\epsilon' - \frac{\epsilon\cdot p\epsilon'\cdot p'}{q\cdot p} - \frac{\epsilon\cdot p'\epsilon'\cdot p}{q\cdot p'}\right), \end{aligned} \tag{13}$$

which are related to those in Eq. (10) by

$$\begin{aligned} A^C(s,t,u) &= 2A(s,t,u) + \frac{B(s,t,u)}{2}\left(\frac{1}{M_\pi^2 - t} + \frac{1}{M_\pi^2 - u}\right),\\ B^C(s,t,u) &= \frac{B(s,t,u)}{4s}\left(\frac{1}{M_\pi^2 - t} + \frac{1}{M_\pi^2 - u}\right). \end{aligned} \tag{14}$$

We have performed several checks on our full expressions: i) in the evaluation, we have fixed neither a specific gauge nor a system of reference, and hence we are able to check explicitly gauge invariance in the results; ii) all nonlocal divergences cancel when adding the full set of diagrams together with wave function renormalization; iii) the polynomial divergences also cancel against the counterterms determined in Ref. [7] $2\gamma_5 = \gamma_6 = \frac{1}{3}(4c_{1d}^2 - 1)$; and iv) once we shift the bare pion mass to the renormalized physical one, the amplitude turns out to be independent of Z_1 and Z_2. In view of these stringent checks, we trust our calculations of the matrix elements.

At this $\mathcal{O}(p^4)$ order, each of the above amplitudes can be split as

[1]To avoid confusion between the low-energy constants in χPT and SχPT, the former are denoted by l_i, while the latter are denoted by ℓ_i. The ℓ_i constants become l_i in the absence of S_1. As is customary in χPT, the finite and scale-independent terms of ℓ_i (l_i) are denoted by $\bar{\ell}_i$ ($\bar{l}_i$).

$$A(s,t,u) = \left[\frac{1}{F^2}\{2(2\ell_5 - \ell_6) + \bar{G}(s)\}\right] + \frac{c_{1d}^2}{F^2}\tilde{A}_s(s,t,u) + \frac{c_{1d}c_{1\gamma}}{F^2}\tilde{A}_{\gamma\gamma}(s,t,u),$$
$$B(s,t,u) = [2] + \frac{c_{1d}^2}{F^2}\tilde{B}_s(s,t,u). \quad (15)$$

The explicit expressions for the $\tilde{A}_s(s,t,u)$, $\tilde{B}_s(s,t,u)$, and $\tilde{A}_{\gamma\gamma}(s,t,u)$ terms are gathered in the Appendix. The contributions in squared brackets correspond to χPT [13]. Notice that corrections to $B(s,t,u)$ at $\mathcal{O}(p^4)$ are absent in χPT and only show up at higher orders [14]. This confirms, as previously remarked in Ref. [7], that the value for observables in SχPT at $\mathcal{O}(p^4)$ lie within the $\mathcal{O}(p^4)$ and $\mathcal{O}(p^6)$ results in χPT.

IV. RESULTS

To extract the value of the $\gamma\gamma S_1$ coupling constant, we have simultaneously fitted the experimental central values of the data for the processes $\pi \to \pi\gamma, \gamma\gamma \to \pi^0\pi^0$, and $\gamma\gamma \to \pi^+\pi^-$. For the latter, we only took into account the data points in Ref. [15] near the two-pion production, $\sqrt{s} \approx 0.45$ MeV; this removes to a large extent the $K\bar{K}$ effects. The data treatment of the former two experiments is described at length in Ref. [7]. In all the procedures, the only new free parameter, besides $c_{1\gamma}$, at play with respect to those entering in Ref. [7] is the low-energy constant ℓ_5. We have generated a sufficient refined lattice for the set of constants, 5×10^6 points, in the hyperplane defined by $\{c_{1d}, M_\sigma, \Gamma', \ell_\Delta, \bar{\ell}_6, c_{1\gamma}\}$[2] with *a priori* flat distribution and computed their corresponding χ^2 augmented function. Notice that we have treated all the coupling constants entering in the processes at the same footing, i.e., without imposing *a priori* any hierarchy, and nevertheless the output is consistent with the assumed counting power, $|c_{1\gamma}| \ll |c_{1d}|$. The main result of this fit is given by

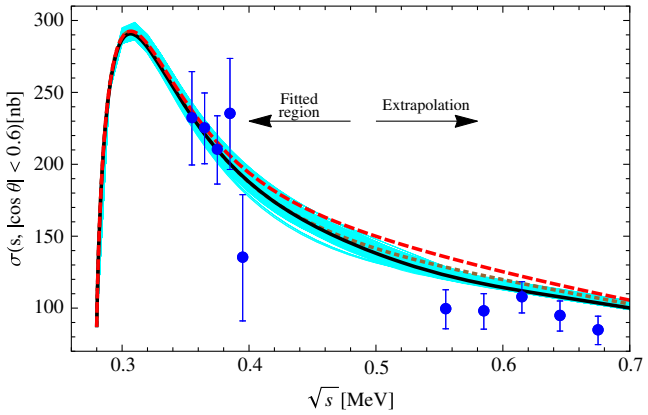

FIG. 1 (color online). $\gamma\gamma \to \pi^+\pi^-$ cross section vs the center-of-mass energy. The full line corresponds to the input values obtained in our fit as described in the main text (16), and the dashed line corresponds to χPT at $\mathcal{O}(p^4)$. The dotted line corresponds to the results for the singlet obtained in Ref. [17] where, in addition to those, we fitted the value of $2\ell_5 - \ell_6 = 0.0030$. We used data values below 0.5 MeV for our fit, while the rest of the curve is just extrapolated.

$$c_{1d} = 0.26^{+0.10}_{-0.07}, \qquad \ell_\Delta = 2\ell_5 - \ell_6 = 0.0026^{+0.0015}_{-0.0004}, \qquad \bar{\ell}_6 = 19.8^{+10}_{-2.9},$$
$$M_\sigma = 553^{+46}_{-114}\ \text{MeV}, \qquad \Gamma' = 295^{+229}_{-157}\ \text{MeV}, \qquad c_{1\gamma} = -0.012^{+0.016}_{-0.010} \quad (16)$$

and is depicted in Fig. 1 as the full curve for the $\gamma\gamma \to \pi^+\pi^-$ cross section. Fits to $\gamma\gamma \to \pi^0\pi^0$ and $\pi \to \pi\gamma$, not shown here, are similar to those obtained in Ref. [7]. The total $\chi^2_{\text{d.o.f}}$ for the joint fit of all the three processes is $\frac{180.4}{69}$. For comparison, the same fit but using χPT at $\mathcal{O}(p^4)$ gives $\chi^2_{\text{d.o.f}} = \frac{361.4}{65}$. Notice that the finding concerning $c_{1\gamma}$ matches the short-distance arguments that suggest a small two-photon coupling [16]. Errors in Eq. (16) correspond to the 1σ deviations. It is worth emphasizing that the narrow thickness of the band in Fig. 1 suggests that this experiment is not suitable to pin down the scalar mass and/or width. This statement is more evident if we compare our outputs for the singlet mass and width (16) to those obtained in Ref. [17], $M_\sigma = 420$ MeV and $\Gamma' = 286$ MeV.[3] The latter, depicted as the dotted line in Fig. 1, lies within the 1σ deviation from the central value of Eq. (16). It is also worth emphasizing that a tiny variation in the fit, for instance, including or not the data point at $\sqrt{s} = 0.395$ MeV, changes the preferable $\{M_\sigma, \Gamma'\}$ set point that minimizes the data.

The value of the combination of low-energy constants must be compared to those standard estimates obtained in Ref. [14], $2l_5 - l_6 = 0.0028$ and Ref. [18], $2l_5 - l_6 = 0.0031$, or to that extracted independently from the $\pi^+ \to e^+\mu_e\gamma$ decay via the axial–vector-to-vector form factor ratio $\frac{h_A}{h_V}$, $2l_5 - l_6 = 0.0031$ [19]. The difference between those results and the corresponding one in Eq. (16) gives an

[2]Notice that ℓ_Δ is finite and scale independent. It can be expressed in terms of $\bar{\ell}_i$ quantities as $\ell_\Delta = -\frac{1}{96\pi^2}\bar{\ell}_\Delta = -\frac{1}{96\pi^2}(\bar{\ell}_5 - \bar{\ell}_6)$.

[3]We have rewritten the outputs of Ref. [17] (where mass and width were defined as $s_\sigma = (M_\sigma - i\frac{\Gamma'}{2})^2$) in our convention as $s_\sigma = M_\sigma^2 - i\Gamma' M_\sigma$.

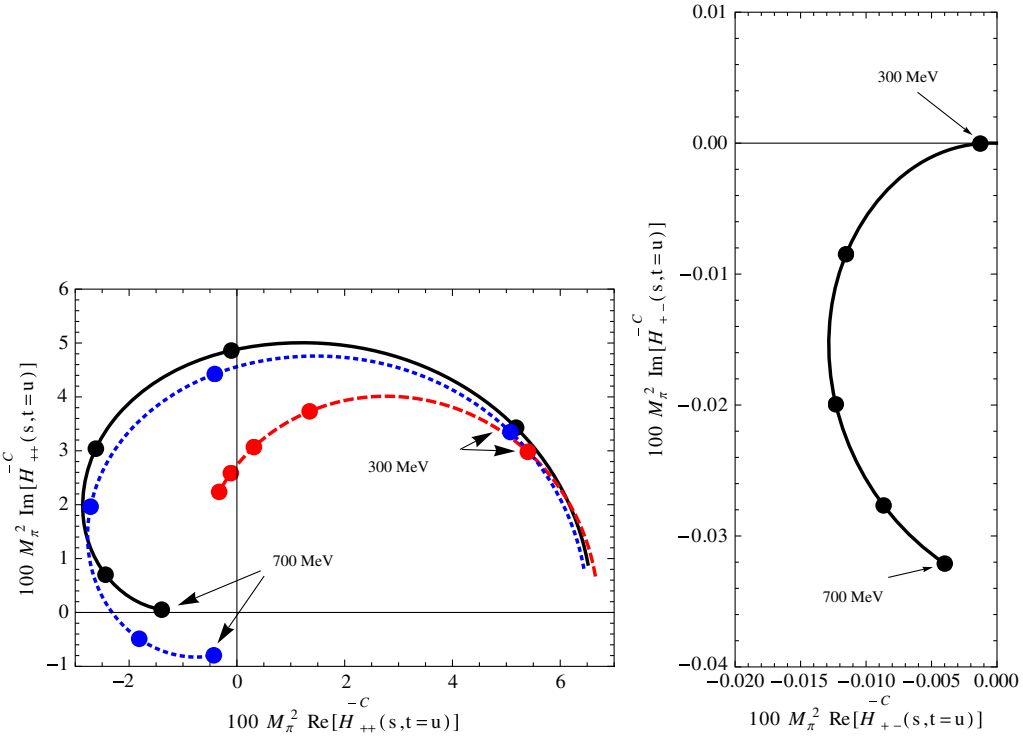

FIG. 2 (color online). Imaginary vs real (Argand plot) parts of the Born subtracted $\mathcal{O}(p^4)$ helicity amplitudes, $\bar{H}^C_{++}(s,t=u)$ and $\bar{H}^C_{+-}(s,t=u)$, as a function of the center-of-mass energy. The solid line is obtained using the central values in Eq. (16). The dotted curve is as above but with the electromagnetic coupling set to zero. Finally, the dashed line corresponds to the χPT case. The dots signal the center-of-mass energy of the two-pion system in 100 MeV steps. Notice that $\bar{H}^C_{+-}$ does not receive any contribution from χPT at $\mathcal{O}(p^4)$. Also, the dashed line is indistinguishable from the solid line in this latter case.

understanding of the effect of the singlet field in this combination of low-energy constants. As was expected from the beginning, the contribution of the scalar singlet is mild in this process because it is mainly saturated by vectors and axials.

In Fig. 2, we plot the imaginary vs the real parts of the helicity amplitudes at $t=u$ once the Born contribution is subtracted:

$$\bar{H}^C_{++} \coloneqq H^C_{++} - H^C_{B++}, \qquad \bar{H}^C_{+-} \coloneqq H^C_{+-} - H^C_{B+-}. \tag{17}$$

It is evident that the electromagnetic correction is small and that at large energies there are a relatively large enhancement, with respect to the χPT, due to the inclusion of the scalar particle.

For completeness, we have also evaluated the dipole polarizabilities of the charged pion. This is obtained via the Compton scattering process $\gamma\pi^+ \to \gamma\pi^+$, which is related to the pion-pair production by crossing symmetry $s \leftrightarrow t$. Expanding (17) at the Compton threshold and using the input (16), we obtained

$$\begin{aligned}(\alpha_1-\beta_1)_{\pi^+} &\cong (4.0^{+2.3}_{-1.3},\quad [6.0],\quad \{5.7\})\times 10^{-4}\ \mathrm{fm}^3,\\ (\alpha_1+\beta_1)_{\pi^+} &\cong (0.012^{+0.011}_{-0.006},\quad [0],\quad \{0.16\})\times 10^{-4}\ \mathrm{fm}^3,\end{aligned} \tag{18}$$

where the numbers in square (curly) brackets stand for the standard χPT values at $\mathcal{O}(p^4)$ [$\mathcal{O}(p^6)$]. As in the χPT case, it seems very hard to reconciliate the sharp discrepancy of Eq. (18) with the most recent experimental result based on the radiative pion photoproduction, $\gamma p \to \gamma\pi^+ n$, $(\alpha_1-\beta_1)^{\mathrm{exp}}_{\pi^+} = (11.6 \pm 1.5_{\mathrm{stat}} \pm 3.0_{\mathrm{syst}} \pm 0.5_{\mathrm{mod}}) \times 10^{-4}\ \mathrm{fm}^3$ [20].

V. REVISITING $\Gamma(S_1 \to \gamma\gamma)$

We are now in a position to find the decay width of the scalar singlet to two photons. This was partially treated in Ref. [7] with the proviso that its direct coupling to photons was suppressed and the bulk of the contribution comes from the radiative process. Relaxing the above assumption and taking the $\gamma\gamma S_1$ term into account, we obtain

$$\Gamma(S_1 \to \gamma\gamma) = \frac{\alpha^2\pi}{4F^2} M_\sigma^3 \left| c_{1\gamma} - 8c_{1d}\frac{M_\sigma^2 - 2M_\pi^2}{M_\sigma^2}\bar{G}(M_\sigma^2)\right|^2 \cong 0.126^{+0.349}_{-0.044}\ \mathrm{keV}. \tag{19}$$

TABLE I. Comparison for $\Gamma(S_1 \to \gamma\gamma)$ between different models.

Reference	$\Gamma(S_1 \to \gamma\gamma)$ (keV)
This work	$0.126^{+0.349}_{-0.044}$
[3]	2.8
[22]	1.68 ± 0.15
[23]	2.08 ± 0.20
[24]	$1.4 \sim 3.2$
[25]	3.08
[26]	2.08
[27]	1.7 ± 0.4
[28]	1.2 ± 0.4
[29]	4
[30] model A	3.5 ± 0.7
[30] model B	2.4 ± 0.5
[31]	≤ 1

TABLE II. Comparison for an $SU(3)$ extension of $\Gamma(S_1 \to \gamma\gamma)$ using a naive extrapolation for the low-energy constants.

$r_{\sigma K\pi}$	1 [universality]	0.8 [3]	0.37 [24]	0.62 [26]
$\Gamma(S_1 \to \gamma\gamma)$ (keV)	0.134	0.132	0.128	0.130

Notice that in the previous expression both terms, Born and radiative corrections, are of the same effective counting power. Analytically, Eq. (19) agrees with the Born approximation of Ref. [5] once we set $c_{1d} = 0$. It is worth emphasizing the M_σ^3 dependence in the above expression. This makes specially relevant the definition of the mass for a particle with a width comparable to its mass. Had we used the convention in Ref. [17], our prediction for the central value of the scalar mass would have been approximately 3% larger, or, equivalently, the sigma radiative width would have increased by a factor $\simeq 1.1$. This can be accounted for as a source of systematic error.

Owing to the smallness of Eq. (19) in comparison with the characteristic width of a conventional $Q\bar{Q}$ resonance, for instance, $\Gamma(f \to \gamma\gamma) \approx 5$–$6$ keV [21], we can conclude in light of Eq. (3) that S_1 is mainly non-$Q\bar{Q}$. A comparison with other results that can be found in the literature is collected in Table I. One salient point is that ours is roughly a decade lower than the results obtained through dispersive calculations.

Aiming at a further theoretical interpretation, we have checked whether this deviation with respect to the dispersive calculation can be assessed to a strong $\sigma \to K\bar{K}$ coupling [25]. We have extended our analytical results to $SU(3)$, and for a first and very crude estimation, we took *naively* the values given in Eq. (16) but considering different ratios for the quantity $r_{\sigma K\pi} = \frac{g_{\sigma KK}}{g_{\sigma\pi\pi}}$.[4] By looking at the results, collected in Table II, we may conservatively expect almost no sensitivity in the singlet decay width due to the presence of the strange quark mass.

To cross-check further our full approach, we have computed the $\gamma\gamma \to \pi^+\pi^-$ $I = 0$ s-wave phase shift δ_0^0 in the threshold region. This is related to the $\pi\pi$ elastic scattering phase shifts through Watson's theorem. We have proceeded to reconstruct the partial waves amplitudes, T_l^I, from the neutral and charged $\gamma\gamma \to \pi\pi$ processes and through these the phase shifts. As is customary, we express the $\pi - \pi$ elastic scattering result as the expansion in energy [32],

$$\delta_l^I = \arctan\left(\mathrm{Re}T_l^I\right) + \mathcal{O}(E^6) = \delta_l^{I(2)} + \delta_l^{I(4)} + \mathcal{O}(E^6),$$
$$16M_\pi^2 \geq s \geq 4M_\pi^2. \tag{20}$$

At any time, we bear in mind that the truncated chiral expansion becomes unreliable above $\sqrt{s} \approx 450$ MeV. In Fig. 3, we have depicted our results for the central values (16), adding for comparison the corresponding χPT ones. As is evident from the figure, we obtain a remarkable improvement with respect to the χPT prediction, and the agreement with the most recent data is rather good, especially for the energy range $0.5\,\mathrm{GeV} \leq \sqrt{s} \leq 0.7\,\mathrm{GeV}$. We stress that there is no fit to these data and this is just a *prediction* or a consistency check. This, together with the fact that we reproduce the experimental data for the $\pi - \pi$ scattering lengths, pion polarizabilities, and the pion radii [7] lets us think that we have obtained a fairly good parametrization of the low-energy region containing the effects of the singlet state.

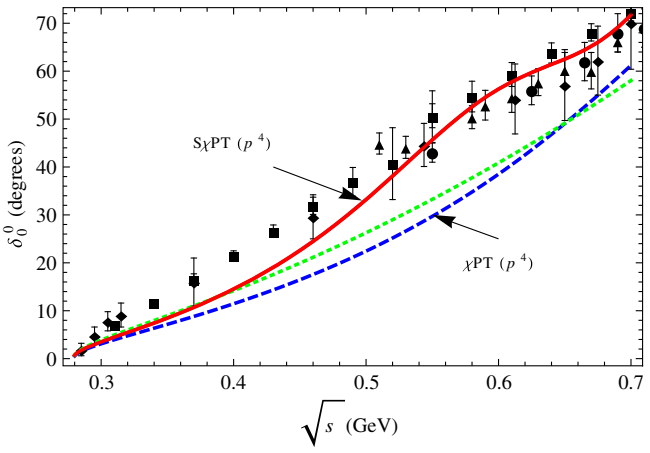

FIG. 3 (color online). $\gamma\gamma \to \pi^+\pi^-$, $I = 0$ s-wave phase shift δ_0^0 in the low-energy region. The keys to experimental data are as follows: (square [33], diamond [34], triangle [35], circle [36]). The blue dashed and red full lines correspond to the $\mathcal{O}(p^4)$ results for χPT and SχPT, respectively. The green dotted line denotes the $\pi\pi$ elastic scattering $\delta_0^{0(2)}$. All curves agree at the threshold, obeying Watson's theorem.

[4] $g_{\sigma\pi\pi}$ stands for the obvious generalization of c_{1d}.

TABLE III. Comparison of different results for the direct contribution to the decay width.

	This work	[3]	[24]	[25]	[37]	[38]	[39]	[40] Fit I	[40] Fit II
$\Gamma_{S_1\to\gamma\gamma}$ (keV)	$0.115^{+0.114}_{-0.115}$	0.13 ± 0.05	0.3	0.16	0.005	0.05–0.1	0.9	0.024 ± 0.023	0.38 ± 0.09

TABLE IV. Comparison of different results for the rescattering contribution to the decay width.

	This work	[3]	[25]	[41]
$\Gamma_{S_1\to\pi\pi\to\gamma\gamma}$ [keV]	$0.194^{+0.282}_{-0.113}$	2.7 ± 0.4	1.89	2

Once we have settled the consistency of the approach, let us come back to the discussion on the quark content. The gluonium or four-quark scenarios are the most controversial scenarios to disentangle from our analysis. To do so, we look at the relative weight between both terms in Eq. (19). Considering just the direct coupling term, one obtains the results in Table III.

Considering instead the decay via the rescattering process, we get the results in Table IV. The difference with the 0.11 keV value found in Ref. [7] is due to the slightly bigger value of c_{1d}. Thus, the initial mismatch with the dispersive calculation can be traced back to the rescattering term.

In particular, the difference can have a twofold origin [see Eq. (19)]:

(i) *The constant* c_{1d}.—Although this constant is estimated at tree level, its value is essentially upper bounded by the pion vector form factor and the $I = 0$ s-wave phase shift δ_0^0 below the $K\bar{K}$ threshold. One expects that the value is renormalized and at the scale μ is enhanced by a factor $\log(\frac{M_\pi^2}{\mu^2})$.

(ii) *The* $\bar{G}(M_\sigma^2)$ *function, or more generically pion rescattering effects*.—Notice that, due to counting power contributions to $\Gamma_{S_1\to\gamma\gamma}$ starting already at $\mathcal{O}(p^4)$, one expects higher-order corrections of $\approx 20\% \sim 30\%$. To estimate these, we have partially resummed a subset of higher-order diagrams obtaining an increase of $\sim 10\%$ with respect to the central value in Eq. (19). Thus, although this result is incomplete, this seems to indicate that the numerical differences with respect to the dispersive results are hard to be obtained by higher-order corrections.

On the other side, one has to bear in mind that dispersive calculations are not free of uncertainties. We mention a few instances in the following:

(i) The results seem to be very sensible to the matrix element parametrization above the $K\bar{K}$ threshold.

(ii) Only the s-wave component is kept at low energy.

(iii) The result seems to be very sensitive to the actual value of the analogous of c_{1d}, i.e., $g_{\sigma\pi\pi}(s)$.[5] For instance, the differences between the value [24,26], given in Table I, and those found in Ref. [42], $0.2 \sim 0.3$ keV, are just due to the value of this coupling.

(iv) The approach, by analytical continuation, evaluates the matrix element deep in the complex plane. One has to keep in mind that the original embedding [43] is valid for matrix elements evaluated close to the real axis.

Comparing the central value for the direct and rescattering decay widths, we learn that the relative weight between both terms in Eq. (19) is approximately 1:2 and that their interference is partially destructive. The relative smallness of the direct coupling in front of the radiative term, mediated via pion loops, can be interpreted as an indication of a dominant $Q^2\bar{Q}^2$ component in the nature of the scalar singlet. However, this conclusion has to be taken cautiously as we have checked that for an increasing singlet mass the scenario can be reversed. Obviously, all the above reflections are in the absence of mixing, which can obscure this simple picture. In fact, this is neither strange nor new, as similar conclusions are supported by QCD sum rules [2], lattice QCD calculations [44], and large-N_c scaling arguments [45]. The novelty of our approach resides in the fact that this finding is encoded in the low-energy regime and an effective approach suffices to capture it.

VI. CONCLUSIONS

We have found an estimate for the scalar-to-two-photons decay width using low-energy data. The fact that the preferred point is attained for $|c_{1\gamma}| < 1$ but is nonvanishing signals the presence of the canonical anomaly [16]. Making use of the central values of Eq. (16) together with Eq. (2), and $R = \frac{5}{3}$ for consistency, we obtain $F_{S_1} \approx -2.3F_\pi$, to be compared with the $Q\bar{Q}$ and the pure glueball results: $F_{S_1} = -F_\pi$ and $F_{S_1} \approx -5F_\pi$, respectively [5]. This fact reinforces our conclusions about the tetraquark nature of the scalar meson as derived from its coupling to two photons (19).

Adopting the most optimistic attitude, i.e.: (i) taking into account higher order resummations, (ii) including $SU(3)$ extensions, and (iii) considering the sensitivity of the results on c_{1d} and M_σ, the central value in Eq. (19) could be pushed up to

$$\Gamma(S_1 \to \gamma\gamma) \approx (0.3 \sim 0.4)\ \text{keV}. \tag{21}$$

This agrees with other effective approaches, studies of the low-energy data using a Breit–Wigner cross section, or

[5]Not to be confused with the energy-independent generalization of c_{1d} used in Table II.

studies of the $\gamma\gamma \to \pi^0\pi^0$ cross section assuming scalar dominance [46]. Still, there is a mismatch of a factor $4 \sim 5$ with respect to the dispersive approaches.

Concerning the possible sources of the difference with respect to the dispersive calculations, two comments are in order:

(i) We have an analytic expression for the rescattering piece at $\mathcal{O}(p^4)$. We remind the reader that within the effective framework unitarity is only satisfied perturbatively, contrary to the dispersive approach in which unitary is enforced by construction and the use of high-energy data is taken into account. This is also the main reason underlaying the small deviation from the scattering phase shifts data below 0.5 GeV as in the standard case [48].

(ii) Concerning the second source, the coupling c_{1d} has a more controversial status. Being a tree level constant, we have estimated it using processes for which its role enters at the next-to-leading level. Due to the sensitivity in the dispersive approach to the value of $g_{\sigma\pi\pi}(s)$ it would be interesting to have a constraint on c_{1d} coming from processes where it plays a dominant role even at leading order.

We stress that only low-energy data were used in our approach.

ACKNOWLEDGMENTS

P. T. is partially supported by the Spanish Ministry of Science, FPA2013-46570.

APPENDIX $\gamma\gamma \to \pi^+\pi^-$ AMPLITUDE IN SχPT AT $\mathcal{O}(p^4)$

We have gathered in this Appendix all the relevant information concerning the rational functions and integrals appearing in the amplitudes (15), together with the diagrams that describe the process $\gamma\gamma \to \pi^+\pi^-$; see Fig. (4). In the calculation, we used dimensional regularization in the $\overline{\text{MS}}$ scheme.

The short-hand notation of the amplitude can be cast in terms of the finite part of the one-, two-, three-, and four-point scalar functions as

$$\begin{aligned}
&\mathcal{K}_0(s,t,u) = \mu_\pi - \mu_\sigma, \qquad \mathcal{K}_1(s,t,u) = \bar{J}_{\pi\sigma}(M_\pi^2), \qquad \mathcal{K}_2(s,t,u) = \bar{J}_{\pi\sigma}(t),\\
&\mathcal{K}_3(s,t,u) = \bar{G}(s), \qquad \mathcal{K}_4(s,t,u) = \bar{C}_0(s, M_\pi^2, M_\pi^2, M_\pi^2, M_\pi^2, M_\sigma^2),\\
&\mathcal{K}_5(s,t,u) = \bar{C}_0(0, t, M_\pi^2, M_\pi^2, M_\pi^2, M_\sigma^2),\\
&\mathcal{K}_6(s,t,u) = \bar{D}_0(0, 0, M_\pi^2, M_\pi^2, s, t, M_\pi^2, M_\pi^2, M_\pi^2, M_\sigma^2),
\end{aligned} \tag{A1}$$

where the $\bar{C}_0$ and $\bar{D}_0$ functions are the ones introduced in Ref. [49] and the overline indicates that they incorporate the $\frac{1}{16\pi^2}$ factors, as the $\bar{J}$ and $\bar{G}$ functions do. In particular,

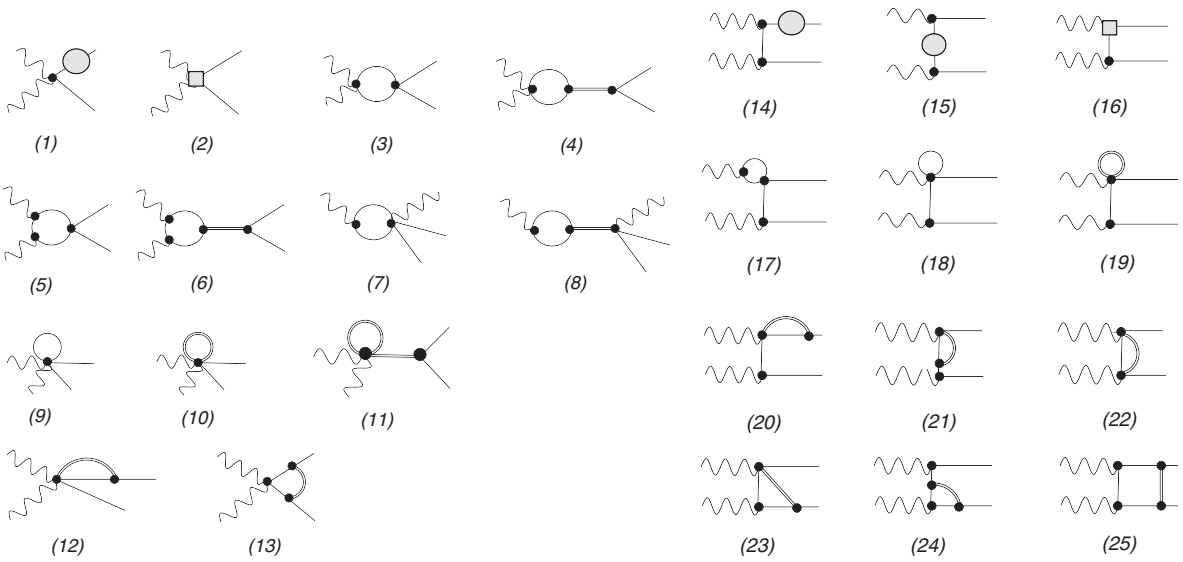

FIG. 4. Feyman diagrams for the process $\gamma\gamma \to \pi^+\pi^-$. The keys to the states are as follows: wavy lines = photons, full lines = pions, and double full lines = scalar singlet. Diagrams from (1)–(13) denote the s-channel, and they contribute to the $\epsilon \cdot \epsilon'$ component of the amplitude. The t (u)-channel, diagrams (14)–(25), contribute to the transverse components of the amplitude.

$$\bar{G}(s) \coloneqq -\left[\frac{1}{16\pi^2} + 2M_\pi^2 \bar{C}_0(0,0,s,M_\pi^2,M_\pi^2,M_\pi^2)\right]. \tag{A2}$$

We can split the amplitudes in terms of a polynomial piece and a dispersive one as

$$\begin{aligned}
\tilde{A}_s(s,t,u) &= \left[P_A(s,t,u) + \sum_{i=0}^{6} U_{Ai}(s,t,u)\mathcal{K}_i(s,t,u)\right] + [t \leftrightarrow u],\\
\tilde{B}_s(s,t,u) &= \left[P_B(s,t,u) + \sum_{i=0}^{6} U_{Bi}(s,t,u)\mathcal{K}_i(s,t,u)\right] + [t \leftrightarrow u],
\end{aligned} \tag{A3}$$

where the $\mathcal{K}'$ s correspond to the scalar loop functions and U' s are rational functions of the masses, scalar width, and Mandelstand variables, with $\nu = t - u$. The terms contributing to the $\tilde{A}_s(s,t,u)$ contribution are

$$\begin{aligned}
P_A(s,t,u) &= \frac{s(M_\sigma^2 - 2M_\pi^2)^2(2M_\sigma^2 - 4M_\pi^2 + s)}{16\pi^2(M_\pi^4 - tu)^2},\\
U_{A0}(s,t,u) &= 0,\\
U_{A1}(s,t,u) &= \frac{4(M_\sigma^2 - 2M_\pi^2)^2(M_\pi^4 s + 2M_\pi^2 tu - 2M_\pi^6 + stu)}{s(t - M_\pi^2)(M_\pi^2 - u)(tu - M_\pi^4)},\\
U_{A2}(s,t,u) &= -\frac{8t(M_\sigma^2 - 2M_\pi^2)^2(M_\pi^2 - u)}{s(t - M_\pi^2)(M_\pi^4 - tu)},\\
U_{A3}(s,t,u) &= \frac{1}{8s(M_\pi^4 - tu)^2}[16M_\pi^4 s(10sM_\sigma^2 + s^2 + 2\nu^2) - 2M_\sigma^2(s^2 - \nu^2)^2 + s(s^2 - \nu^2)^2\\
&\quad + 8s^3 M_\sigma^4 + 16s^2 M_\sigma^6 - 64M_\pi^6 s^2 - 4M_\pi^2(24s^2 M_\sigma^4 + 4sM_\sigma^2(s^2 + \nu^2) + s^4 - \nu^4)]\\
&\quad - 4(s - 2M_\pi^2)^2 \frac{F(s)}{s},\\
U_{A4}(s,t,u) &= -\frac{2M_\pi^2(M_\sigma^2 - 2M_\pi^2)^2(-2M_\pi^4 + t^2 + u^2)}{(M_\pi^4 - tu)^2},\\
U_{A5}(s,t,u) &= -\frac{8M_\pi^2(M_\sigma^2 - 2M_\pi^2)^2(M_\pi^2 - t)(-M_\sigma^2 + M_\pi^2 + t)}{(M_\pi^4 - tu)^2},\\
U_{A6}(s,t,u) &= -\frac{4M_\pi^2(M_\sigma^2 - 2M_\pi^2)^2}{s(M_\pi^4 - tu)^2}[s^2 M_\sigma^4 + M_\pi^4(s^2 - 12t^2) - 2s^2 M_\sigma^2(M_\pi^2 + t)\\
&\quad + 2M_\pi^2 t^2(3s + 4t) - 2M_\pi^6(s - 4t) - 2M_\pi^8 - t^2(s^2 + 4st + 2t^2)],
\end{aligned}$$

and the terms contributing to the $\tilde{B}_s(s,t,u)$ amplitude read

$$\begin{aligned}
P_B(s,t,u) &= \frac{-(M_\sigma^2 - 2M_\pi^2)^2}{16\pi^2 M_\pi^2(4M_\pi^2 - M_\sigma^2)(M_\pi^4 - tu)^2}[4M_\pi^2(M_\pi^2 s^3 + M_\pi^4(-6s^2 + t^2 + u^2) + 8M_\pi^6 s\\
&\quad - 5M_\pi^8 + tu(t^2 + tu + u^2)) + 2sM_\sigma^4(t - M_\pi^2)(M_\pi^2 - u) + s(s - 12M_\pi^2)M_\sigma^2(t - M_\pi^2)(M_\pi^2 - u)],\\
U_{B0}(s,t,u) &= \frac{8M_\pi^2(M_\sigma^2 - 2M_\pi^2)^2}{-5M_\pi^2 M_\sigma^2 + M_\sigma^4 + 4M_\pi^4},
\end{aligned}$$

$$U_{B1}(s,t,u) = \frac{4(M_\sigma^2 - 2M_\pi^2)^2}{M_\pi^2(4M_\pi^2 - M_\sigma^2)(M_\pi^2 - t)(M_\pi^2 - u)(M_\pi^4 - tu)}[-M_\pi^8(M_\sigma^2 + s) + M_\pi^2 tu(2sM_\sigma^2 - 3tu) - 7M_\pi^4 stu + t^2u^2M_\sigma^2 - 2M_\pi^6 tu + 5M_\pi^{10}],$$

$$U_{B2}(s,t,u) = \frac{8(M_\sigma^2 - 2M_\pi^2)^2 t(u - M_\pi^2)}{(t - M_\pi^2)(tu - M_\pi^4)},$$

$$U_{B3}(s,t,u) = \frac{s(M_\sigma^2 - 2M_\pi^2)^2(t - M_\pi^2)(M_\pi^2 - u)(2M_\sigma^2 - 4M_\pi^2 + s)}{M_\pi^2(M_\pi^4 - tu)^2},$$

$$U_{B4}(s,t,u) = \frac{2(M_\sigma^2 - 2M_\pi^2)^2(t - M_\pi^2)(u - M_\pi^2)(-2M_\pi^4 + t^2 + u^2)}{(M_\pi^4 - tu)^2},$$

$$U_{B5}(s,t,u) = \frac{8(M_\sigma^2 - 2M_\pi^2)^2(t - M_\pi^2)^2(M_\pi^2 - u)}{(M_\pi^4 - tu)^2}(-M_\sigma^2 + M_\pi^2 + t).$$

$$U_{B6}(s,t,u) = -\frac{4(M_\sigma^2 - 2M_\pi^2)^2(t - M_\pi^2)(M_\pi^2 - u)}{(M_\pi^4 - tu)^2}[-2M_\pi^2(sM_\sigma^2 + t^2) + s(t - M_\sigma^2)^2 + M_\pi^4(s + 4t) - 2M_\pi^6].$$

Finally, the amplitude proportional to the direct $\sigma\gamma\gamma$ coupling $c_{1\gamma}$ (15) is

$$\tilde{A}_{\gamma\gamma}(s,t,u) = \left(\frac{s}{2} - M_\pi^2\right)F(s). \tag{A4}$$

Notice that in the above expressions we have used a Breit–Wigner representation to regularize the propagator of the scalar particle

$$F(s) = \frac{1}{s - M_\sigma^2 + iM_\sigma\Gamma'}. \tag{A5}$$

This can be, at first sight, slightly controversial. The main two arguments to use this parametrization are as follows:

(i) As in all the processes studied in Ref. [7], in this work, the propagator enters in the highest radiative order, and thus differences between parametrizations would be reflected at least at $\mathcal{O}(p^6)$, beyond our scope. This would drastically change in the case of studying $\pi - \pi$ scattering where already the scalar propagator enters at lowest order.

(ii) In this line, we have recovered the results in Ref. [7], within the 1σ band, using a different parametrization [50]:

$$F(s) = \frac{1}{s - M_\sigma^2 + iM_\sigma\Gamma(s)}, \quad \text{with}$$
$$\Gamma(s) = \left(\frac{s - s_0}{M_\sigma^2 - s_0}\right)^{3/2}\Gamma_0. \tag{A6}$$

[1] For an earlier study, see V. A. Novikov, M. A. Shifman, A. I. Vainshtein, and V. I. Zakharov, In search of scalar gluonium, Nucl. Phys. **B165**, 67 (1980).

[2] T. V. Brito, F. S. Navarra, M. Nielsen, and M. E. Bracco, QCD sum rule approach for the light scalars mesons as four-quark states, Phys. Lett. B **608**, 69 (2005).

[3] R. Kaminski, G. Mennessier, and S. Narison, Gluonium nature of the $\sigma/f_0(600)$ from its coupling to $K\bar{K}$, Phys. Lett. B **680**, 148 (2009).

[4] R. L. Jaffe, Multiquark hadrons. I. Phenomenology of $Q^2\bar{Q}^2$ mesons, Phys. Rev. D **15**, 267 (1977).

[5] J. R. Ellis and J. Lanik, Comment on the scalar gluonium decay into two photons, Phys. Lett. B **175**, 83 (1986).

[6] J. Soto, P. Talavera, and J. Tarrus, Chiral effective theory with a light scalar and lattice QCD, Nucl. Phys. **B866**, 270 (2013).

[7] L. Ametller and P. Talavera, The lowest resonance in QCD from low–energy data, Phys. Rev. D **89**, 096004 (2014).

[8] M. Chanowitz and J. Ellis, Canonical trace anomaly, Phys. Rev. D **7**, 2490 (1973).

[9] R. Jaffe and F. Wilczek, Diquarks and exotic spectroscopy, Phys. Rev. Lett. **91**, 232003 (2003).

[10] J. I. Latorre and P. Pascual, QCD Sum rules and the $\bar{q}q\bar{q}q$ system, J. Phys. G **11**, L231 (1985).

[11] J. Lanik, A possible coupling of a scalar glueball to pseudoscalar Goldstone mesons, Phys. Lett. B **144**, 439 (1984).

[12] J. Gasser and H. Leutwyler, Chiral perturbation theory to one loop, Ann. Phys. (N.Y.) **158**, 142 (1984).

[13] J. Bijnens and F. Cornet, Two pion production in photon-photon collisions, Nucl. Phys. **B296**, 557 (1988).

[14] U. Burgi, Charged pion pair production and pion polarizabilities to two loops, Nucl. Phys. **B479**, 392 (1996).
[15] J. Boyer *et al.*, Two photon production of pion pairs, Phys. Rev. D **42**, 1350 (1990).
[16] M. S. Chanowitz and J. R. Ellis, Canonical anomalies and broken scale invariance, Phys. Lett. B **40**, 397 (1972).
[17] I. Caprini, G. Colangelo, and H. Leutwyler, Mass and Width of the Lowest Resonance in QCD, Phys. Rev. Lett. **96**, 132001 (2006).
[18] J. Gasser, M. A. Ivanov, and M. E. Sainio, Revisiting gamma gamma → pi + pi- at low energies, Nucl. Phys. **B745**, 84 (2006).
[19] J. Bijnens and P. Talavera, $\pi \to \ell\nu\gamma$ form-factors at two-loop, Nucl. Phys. **B489**, 387 (1997).
[20] J. Ahrens *et al.*, Measurement of the pi + meson polarizabilities via the gamma p → gamma pi + n reaction, Eur. Phys. J. A **23**, 113 (2005).
[21] S. Krewald, R. H. Lemmer, and F. P. Sassen, Life of Kaonium, Phys. Rev. D **69**, 016003 (2004).
[22] J. A. Oller and L. Roca, Two photons into $\gamma\gamma \to \pi^0\pi^0$, Eur. Phys. J. A **37**, 15 (2008).
[23] B. Moussallam, Coupling of light $l = 0$ scalar mesons to simple operators in the complex plane, Eur. Phys. J. C **C71**, 1814 (2011).
[24] G. Mennessier *et al.*, Can the $\gamma\gamma$ processes reveal the nature of the σ meson?, arXiv:0707.4511.
[25] G. Mennessier, S. Narison, and X. G. Wang, σ and $f_0(980)$ substructures from $\gamma\gamma \to \pi\pi, J/\Psi, \phi$ radiative and D_s semi-leptonic decays, Phys. Lett. B **696**, 40 (2011).
[26] Y. Mao, X.-G. Wang, O. Zhang, H. Q. Zheng, and Z. Y. Zhou, A dispersive analysis on the $f(600)$ and $f(980)$ resonances in $\gamma\gamma \to \pi^+\pi^-, \pi^0\pi^0$ processes, Phys. Rev. D **79**, 116008 (2009).
[27] M. Hoferichter, D. R. Phillips, and C. Schat, Roy-Steiner equations for $\gamma\gamma \to \pi\pi$, Eur. Phys. J. C **71**, 1743 (2011).
[28] J. Bernabeu and J. Prades, The $\sigma \to \gamma\gamma$ Width from Nucleon Electromagnetic Polarizabilities, Phys. Rev. Lett. **100**, 241804 (2008).
[29] J. Babcock and J. L. Rosner, Radiative transitions of low lying positive-parity mesons, Phys. Rev. D **14**, 1286 (1976).
[30] M. R. Pennington, T. Mori, S. Uehara, and Y. Watanabe, Amplitude analysis of high statistics results on $\gamma\gamma \to \pi^+\pi^-$ and the two photon width of isoscalar states, Eur. Phys. J. C **56**, 1 (2008).
[31] F. Giacosa, T. Gusche, and V. E. Lyubovitskij, On the two-photon decay width of the sigma meson, Phys. Rev. **77**, 072001 (2008).
[32] J. Gasser and U. Meißner, On the phase of ϵ', Phys. Lett. B **258**, 219 (1991).
[33] J. R. Batley *et al.* (NA48/2 Collaboration), Precise tests of low energy QCD from (K_{e4}) decay properties, Eur. Phys. J. C **70**, 635 (2010); see the energy-dependent dispersive analysis of the above data as done in R. Garcia-Martin, R. Kamiński, J. R. Peláez, J. Ruiz de Elvira, and F. J. Ynduráin, Pion-pion scattering amplitude. IV. Improved analysis with once subtracted Roy-like equations up to 1100 MeV, Phys. Rev. D **83**, 074004 (2011).
[34] K. M. Mukhin *et al.*, Values of delta00 phases of pi-pi scattering within the range from threshold up to $M_{\pi\pi} = 1$ GeV, Pis'ma Zh. Eksp. Teor. Fiz. **32**, 616 (1980).
[35] P. Estabrooks and A. D. Martin, $\pi - \pi$ phase shifts analysis below the K anti-K threshold, Nucl. Phys. **B79**, 301 (1974).
[36] S. D. Protopopescu, M. Alston-Garnjost, A. Barbaro-Galtieri, S. M. Flatté, J. H. Friedman, T. A. Lasinski, G. R. Lynch, M. S. Rabin, and F. T. Solmitz, $\pi - \pi$ partial waves analysis from reactions $\pi^+ p \to \pi^+\pi^-\Delta^{++}$ and $\pi^+ p \to K^+K^-\Delta{+}{+}$ at 7.1 GeV/c, Phys. Rev. D **7**, 1279 (1973).
[37] N. N. Achasov and G. N. Shestakov, Lightest scalar and tensor resonances in $\gamma\gamma \to \pi\pi$ after Belle experiment, Phys. Rev. D **77**, 074020 (2008).
[38] J. Baacke, T. H. Chang, and H. Kleinert, Compton scattering and the couplings of f, σ, η, A_2 and π to photons and nucleons, Nuovo Cimento A **12**, 21 (1972).
[39] B. Schrempp-Otto, F. Schrempp, and T. F. Walsh, Finite energy sum-rules and the reaction $ee \to ee\epsilon(750)$ and $ee \to eef(1260)$, Phys. Lett. B **36**, 463 (1971).
[40] D. Black, M. Harada, and J. Schechter, Vector Meson Dominance Model for Radiative Decays Involving Light Scalar Mesons, Phys. Rev. Lett. **88**, 181603 (2002).
[41] N. N. Achasov, A. V. Kiselev, and G. N. Shestakov, Theory of scalars, Nucl. Phys. B, Proc. Suppl. **181–182**, 169 (2008).
[42] S. Narison, Masses, decays and mixing of gluonia in QCD, Nucl. Phys. B, Proc. Suppl. **64**, 210 (1998).
[43] R. Omnès, On the solution of certain singular integrals equations of quantum field theory, Nuovo Cimento A **8**, 316 (1958).
[44] M. Alford and R. L. Jaffe, Insight into the scalar mesons from a lattice calculation, Nucl. Phys. **B578**, 367 (2000).
[45] J. R. Pelaez, On the Nature of Light Scalar Mesons from their Large N_c Behaviour, Phys. Rev. Lett. **92**, 102001 (2004).
[46] See comments just above Sec. 3 of Ref. [24] and comments below Eq. (7) in Ref. [47].
[47] M. R. Pennington, Sigma Coupling to Photons: Hidden Scalar in $\gamma\gamma \to \pi^0\pi^0$, Phys. Rev. Lett. **97**, 011601 (2006).
[48] J. F. Donoghue, Dispersion relations and effective field theory, arXiv:hep-ph/9607351.
[49] G. Passarino and M. J. G. Veltman, One loop corrections for e + e− annihilation into mu + mu− in the Weinberg model, Nucl. Phys. **B160**, 151 (1979).
[50] B. Pasquini, D. Drechsel, and S. Scherer, The polarizability of the pion: no conflict between dispersion theory and chiral perturbation theory, Phys. Rev. C **77**, 065211 (2008).